International Journal of Fluid Machinery and Systems
Vol. 2, No. 4, October-December 2009

Original Paper (Invited)

Axisymmetric Swirling Flow Simulation of the Draft Tube Vortex in Francis Turbines at Partial Discharge

Romeo Susan-Resiga[1], Sebastian Muntean[2], Peter Stein[3], and François Avellan[4]

[1]Department of Hydraulic Machinery, "Politehnica" University of Timişoara
Bvd. Mihai Viteazu, No. 1, Timişoara, 300222, Romania
[2]Center for Advanced Research in Engineering Science, Romanian Academy – Timişoara Branch
Bvd. Mihai Viteazu, No. 24, Timişoara, 300223, Romania
[3]VA TECH HYDRO, Hardstasse 319, Zürich, 8005, Switzerland
[4]Laboratory for Hydraulic Machines, École Polytechnique Fédérale de Lausanne
Avenue de Cour 33bis, Lausanne, CH-1007, Switzerland

Abstract

The flow in the draft tube cone of Francis turbines operated at partial discharge is a complex hydrodynamic phenomenon where an incoming steady axisymmetric swirling flow evolves into a three-dimensional unsteady flow field with precessing helical vortex (also called vortex rope) and associated pressure fluctuations. The paper addresses the following fundamental question: is it possible to compute the circumferentially averaged flow field induced by the precessing vortex rope by using an axisymmetric turbulent swirling flow model? In other words, instead of averaging the measured or computed 3D velocity and pressure fields we would like to solve directly the circumferentially averaged governing equations. As a result, one could use a 2D axi-symmetric model instead of the full 3D flow simulation, with huge savings in both computing time and resources. In order to answer this question we first compute the axisymmetric turbulent swirling flow using available solvers by introducing a stagnant region model (SRM), essentially enforcing a unidirectional circumferentially averaged meridian flow as suggested by the experimental data. Numerical results obtained with both models are compared against measured axial and circumferential velocity profiles, as well as for the vortex rope location. Although the circumferentially averaged flow field cannot capture the unsteadiness of the 3D flow, it can be reliably used for further stability analysis, as well as for assessing and optimizing various techniques to stabilize the swirling flow. In particular, the methodology presented and validated in this paper is particularly useful in optimizing the blade design in order to reduce the stagnant region extent, thus mitigating the vortex rope and expending the operating range for Francis turbines.

Keywords: draft tube, vortex rope, turbulent axisymmetric flow, stagnant region model.

1. Introduction

In Francis turbines operated at partial discharge the swirling flow downstream the runner becomes unstable inside the draft tube cone, with the development of a precessing helical vortex (also called vortex rope) and associated severe pressure fluctuations, as exemplified by Escudier [1]. This phenomenon is now well understood and its cause is directly related to the absolute instability of the swirling flow ingested by the turbine's draft tube, Zhang et al. [2]. This conclusion was confirmed Susan-Resiga et al. [3], by performing a stability analysis on an analytical representation of the measured axial and circumferential velocity profiles downstream a Francis runner.

Numerical simulations of the precessing vortex rope have reached the level of accuracy where the main features of the phenomenon (e.g. vortex rope shape, precession frequency, pressure fluctuation) are accurately described, Ruprecht et al. [4], Sick et al. [5], Stein et al. [6], and Ciocan et al. [7]. However, such 3D unsteady turbulent flow computations are very expensive both in terms of computing time and resources. As a result, more computationally tractable techniques are required for performance evaluation and design optimization purposes.

The counter-measures for the rotating vortex rope currently used in practice are most often addressing the effects of the severe flow instability rather than the cause. A novel method for swirling flow control has been introduced by Susan-Resiga et al. [8], where a water

Accepted for publication September 20 2009: Paper number O09028S
Corresponding author: Romeo Susan-Resiga, Professor, resiga@mh.mec.upt.ro

This manuscript was presented at the 24th IAHR Symposium on Hydraulic Machinery and Systems, October 27-31, 2008, Foz do Iguassu-Brazil.

jet is injected from the runner crown tip, and its effectiveness has been proven through 3D unsteady numerical simulation. However, the optimization of the jet parameters (velocity and discharge) requires a far less expensive numerical analysis methodology in order to be used in design practice.

The main goal of this paper is to develop a methodology for analyzing the swirling flows with helical vortex breakdown by using an axisymmetrical swirling flow model. Obviously, the axial symmetry hypothesis is a major simplification having the main benefit of dramatically reducing the computational cost. On the other hand, it introduces important limitations as far as the three-dimensionality and unsteadiness are concerned. Essentially, an axisymmetric flow solver provides a circumferentially averaged velocity and pressure fields, to be further used as a base flow for linear, Olendraru and Sellier [9], or non-linear, Szeri and Holmes [10], stability analysis.

An alternative approach is to use specialized flow solvers in cylindrical coordinates, (e.g. Blackburn [11]), where Fourier expansions in the circumferential direction are used to obtain a set of coupled two-dimensional problems defined for the meridional semi-plane. As a result, the circumferential variation of the flow field, as well as the unsteadiness, could be obtained with computational costs smaller than the full three-dimensional unsteady flow solver, but this approach has not been tested for the complex swirling flows with precessing vortex rope.

The axisymmetric flow field provides a good indicator for the vortex breakdown occurrence and development through the extent of the central quasi-stagnant region, although the unsteady velocity and pressure fluctuations cannot be directly captured. However, based on the theory of helical vortex in a pipe, Alekseenko et al. [12], Kuibin et al. [13] estimate the frequency and amplitude of oscillations caused by the precession of the helical vortex by using four integral characteristics of the axisymmetric steady base flow: vortex intensity, liquid flow rate, and moment and moment of momentum fluxes.

Usually, when employing a simplified flow model one has to check that the model assumptions are in reasonable agreement with the actual flow. In our case, although we are dealing with a swirling flow in an axisymmetrical geometry (the draft tube cone) the inherent flow instability leads to a fully three-dimensional unsteady flow field with precessing vortex rope when the Francis turbine is operated at partial discharge. As a result, the axial symmetry assumption is obviously violated. One can only conjecture that an axisymmetrical flow model can represent the circumferentially averaged three-dimensional unsteady flow. It is this conjecture we investigate in the present paper. In other words, instead of circumferentially averaging the 3D unsteady computational results we would like to perform the circumferentially average on the governing equations in cylindrical coordinates, thus solving a 2D problem in a meridian half-plane. The results obtained with an axisymmetrical turbulent swirling flow model are compared and validated with Laser Doppler Velocity measurements for axial and circumferential velocity profiles, Ciocan et al. [7], as well as with Particle Image Velocimetry investigations of the vortex rope shape, Iliescu et al. [14].

2. Axisymmetric Swirling Flow Model

In order to perform an axisymmetric flow simulation, an equivalent axisymmetric computational domain must be considered. Given the three-dimensional geometry of the actual draft tube investigated in the FLINDT project, Avellan [15], where only the cone is geometrically axisymmetric, we have considered the domain shown in Figure 1 with the radius computed as equivalent as the equivalent hydraulic radius where the cross-section shape is no longer circular. The upstream part of the domain (shown in light blue) corresponds to the actual draft tube cone, while the downstream part corresponds to the elbow, up to the pier.

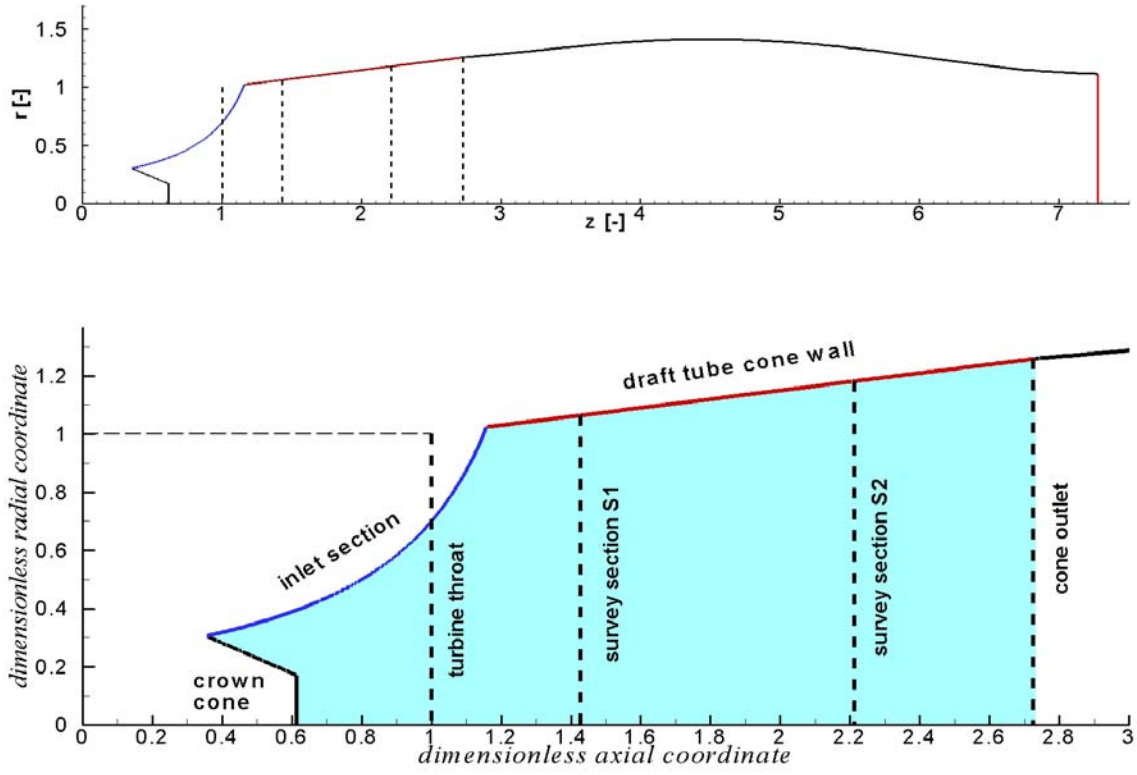

Fig. 1 Computational domain in a meridian half plane.

All lengths are made dimensionless with respect to the turbine throat radius R_{throat}, and the coordinate system origin is chosen such that the throat dimensionless abscissa is equal to unity. The inlet section for the computational domain is located just downstream the runner blade trailing edge. The actual draft tube cone region is shown in detail in Figure 1, and it corresponds to the domain used by Stein et al. [6] for 3D unsteady flow simulation with vortex rope. The cone length is $\sqrt{3}R_{\text{throat}}$, and the cone half-angle is 8.5°. Two survey sections are also shown in Figure 1, where the axial and circumferential velocity profiles were measured using Laser Doppler Velocimetry, Avellan [15], Ciocan et al. [7], further denoted in this paper as S1 and S2. The computational domain is discretized with 90,000 quadrilateral cells, using a boundary layer mesh near the wall.

The circumferentially averaged velocity components and turbulence quantities correspond to the data from Stein et al. [6], Figure 2, for a partial discharge operating point $Q/Q_{opt} = 0.692$. The meridian velocity component is defined as $V_m = \sqrt{V_z^2 + V_r^2}$, and the absolute/relative flow angles are $\alpha = \arctan\left(V_m / V_\theta\right)$ and $\beta = \arctan\left[V_m / \left(\Omega r - V_\theta\right)\right]$, respectively, with V_z, V_r, V_θ the axial, radial and circumferential velocity components, Ω the runner angular velocity. The velocity is made dimensionless with respect to $\sqrt{2gH}$, where H is the turbine head. Avellan [16] relates the increase in both meridian and circumferential velocity components near the band, Figure 2, to the secondary flow in the blade channel, at part load, with the development of a so-called interblade vortex.

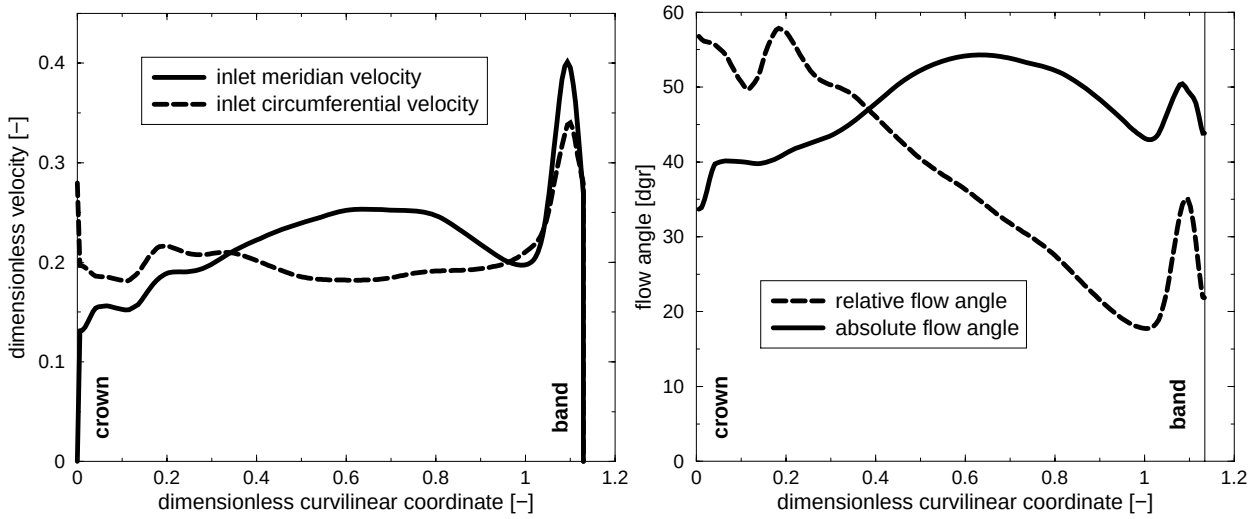

Fig. 2 Velocity profile (left) and flow angle (right) on the inlet section of the computational domain from Figure 1, with curvilinear coordinate running from crown to band.

The swirl number,

$$Sw \equiv \left(\int_{\text{inlet}} r V_\theta \boldsymbol{V} \cdot \boldsymbol{n} \mathrm{d}S \right) \Bigg/ \left(R_{\text{inlet}} \int_{\text{inlet}} V_m \boldsymbol{V} \cdot \boldsymbol{n} \mathrm{d}S \right), \tag{1}$$

has a rather large value, $Sw = 0.64$, and as a result one should expect vortex breakdown to occur downstream into the turbine discharge cone.

On the outlet section we use the radial equilibrium condition which relates the radial pressure gradient with the circumferential velocity,

$$\frac{\partial p}{\partial r} = \frac{\rho V_\theta^2}{r}. \tag{2}$$

The governing equations for axisymmetric swirling flow of an incompressible fluid are:

Continuity equation (divergence free velocity field),

$$\nabla \cdot \mathbf{V} \equiv \frac{\partial V_z}{\partial z} + \frac{\partial V_r}{\partial r} + \frac{V_r}{r} = 0, \tag{3}$$

Axial momentum equation,

$$\frac{\partial V_z}{\partial t} + \frac{1}{r}\frac{\partial}{\partial z}\left(r V_z V_z\right) + \frac{1}{r}\frac{\partial}{\partial r}\left(r V_r V_z\right) = -\frac{1}{\rho}\frac{\partial p}{\partial z} + \frac{1}{r}\frac{\partial}{\partial z}\left[r \frac{\mu + \mu_T}{\rho} 2 \frac{\partial V_z}{\partial z} \right] + \frac{1}{r}\frac{\partial}{\partial r}\left[r \frac{\mu + \mu_T}{\rho} \left(\frac{\partial V_z}{\partial r} + \frac{\partial V_r}{\partial z} \right) \right], \tag{4}$$

Radial momentum equation,

$$\frac{\partial V_r}{\partial t} + \frac{1}{r}\frac{\partial}{\partial z}\left(r V_z V_r\right) + \frac{1}{r}\frac{\partial}{\partial r}\left(r V_r V_r\right) = -\frac{1}{\rho}\frac{\partial p}{\partial r} + \frac{V_\theta^2}{r} + \frac{1}{r}\frac{\partial}{\partial z}\left[r \frac{\mu + \mu_T}{\rho} \left(\frac{\partial V_r}{\partial z} + \frac{\partial V_z}{\partial r} \right) \right] + \frac{1}{r}\frac{\partial}{\partial r}\left[r \frac{\mu + \mu_T}{\rho} 2 \frac{\partial V_r}{\partial r} \right] - 2 \frac{\mu + \mu_T}{\rho} \frac{V_r}{r^2}, \tag{5}$$

Circumferential momentum equation,

$$\frac{\partial V_\theta}{\partial t}+\frac{1}{r}\frac{\partial}{\partial z}\left(rV_zV_\theta\right)+\frac{1}{r}\frac{\partial}{\partial r}\left(rV_rV_\theta\right)=-\frac{V_rV_\theta}{r}+\frac{1}{r}\frac{\partial}{\partial z}\left[r\frac{\mu+\mu_T}{\rho}\frac{\partial V_\theta}{\partial z}\right]+\frac{1}{r^2}\frac{\partial}{\partial r}\left[r^3\frac{\mu+\mu_T}{\rho}\frac{\partial}{\partial r}\left(\frac{V_\theta}{r}\right)\right]. \qquad (6)$$

Obviously, the radial equilibrium condition, eq. (2), follows from the radial momentum equation (5) for vanishing radial velocity. The effective dynamic viscosity is written as the sum of the molecular μ, and the so-called "turbulent" viscosity μ_T, the second one being computed using various turbulence models. The above axisymmetric swirling flow model, which is implemented in the FLUENT 6.3 code, is used for the present computations together with the realizable k-ε (RKE) turbulence model. The term "realizable" means that the model satisfies certain mathematical constraints on the Reynolds stresses, consistent with the physics of the flow. When compared with the standard k-ε and RNG k-ε models, the RKE model is predicting more accurately the spreading rate of both planar and round jets. Shih et al [17] argue that the RKE turbulence model is also likely to provide superior performance for flow involving rotation, boundary layers under strong adverse pressure gradients, separation and recirculation.

One important issue to be addressed is the effect of neglecting the actual precessing vortex rope when computing directly the circumferentially averaged flow. Both experimental data (e.g. Nishi et al. [18], Kirschner and Ruprecht [19]), and theoretical models (e.g. Keller et al. [20]), suggest that when a vortex breakdown occurs a quasi-stagnation region is developed near the axis. This stagnant region must be understood as the average of the highly fluctuating flow field inside the vortex rope. As a result, we have enforced a stagnation condition on top of the FLUENT axisymmetric flow solver whenever a negative (i.e. upstream oriented) axial velocity occurs. The actual implementation of the above Stagnant Region Model (SRM) is done via the User Defined Function presented in the Appendix.

3. Numerical Results and Validation

The numerical computations are performed for the benchmark case investigated in the FLINDT project, where experimental data are available for validation [7], [14], with the computational domain and boundary conditions presented in Section 2.

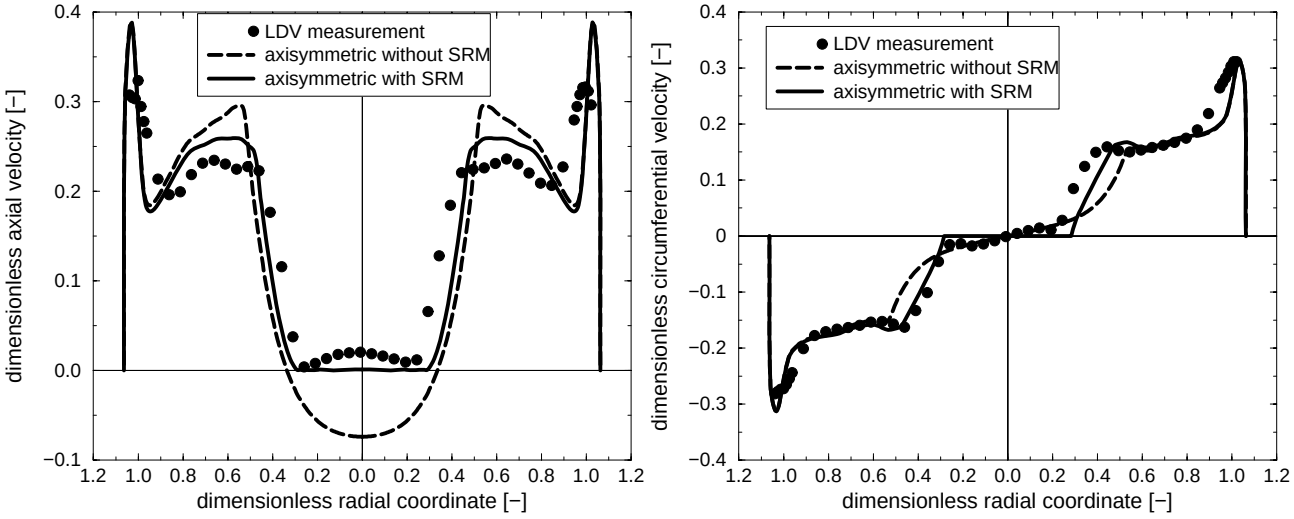

Fig. 3 Axial (left) and circumferential (right) velocity profiles on the upstream survey section S1.

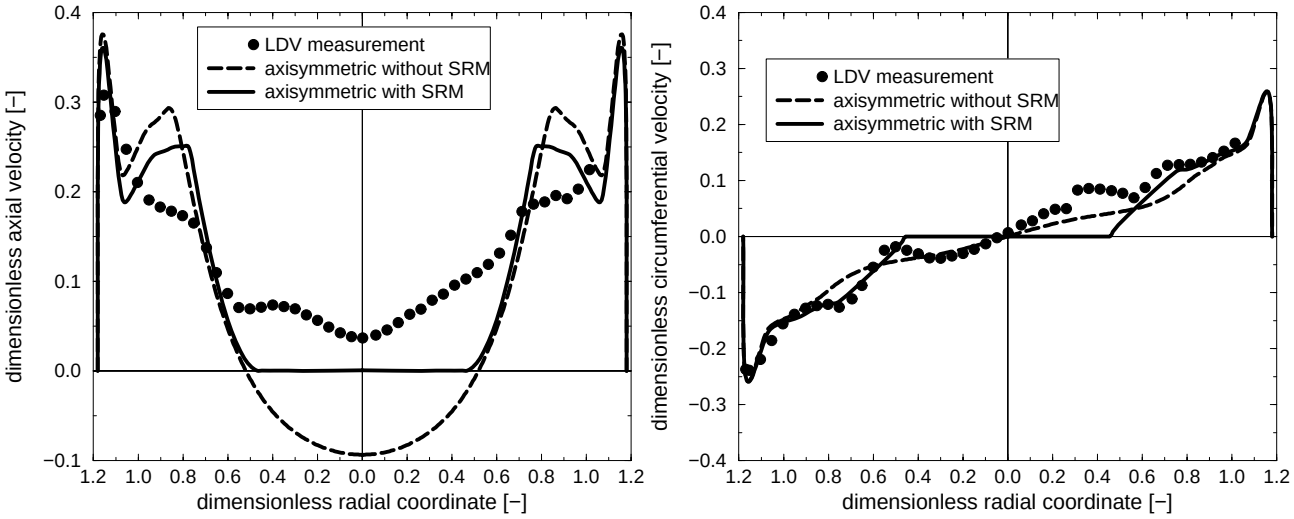

Fig. 4 Axial (left) and circumferential (right) velocity profiles on the upstream survey section S2.

The plain axisymmetric turbulent swirling flow model produces a central recirculation, with the main flow occupying an annular section up to the wall. The axial and circumferential velocity profiles in the survey sections S1 and S2 are shown with dashed lines in Figures 3 and 4, respectively. The axial velocity in section S1 displays a backflow in the central region, which leads to an overestimation of the velocity on the mean flow side of the strong shear flow region. The radial location of the shear flow region is also shifted to larger radii, but the shift is no larger than 0.1 dimensionless. The circumferential velocity in section S1 agrees well with measured data, with the same observation that the shear flow region is predicted at larger radii than measured. As far as the comparison in section S2 is concerned, Figure 4, one should keep in mind that, for the real draft tube, this section is quite close to the elbow, where the axial-symmetry assumption for the wall shape is obviously no longer valid. The large backflow region in the axial velocity profile (dashed line) is in disagreement with the experimental data.

When the Stagnant Region Model (SRM) is activated, the agreement with experimental data is improved, as shown with solid lines in Figures 3 and 4. The axial velocity profile in survey section S1, Figure 3, shows that the radial extent of the shear flow region decreases and it is closer to the experiment. The overestimation of the axial velocity in the main flow at the boundary of the shear flow is reduced, and overall the axisymmetric flow computation with SRM agrees better with the experiment. The same conclusion holds for the circumferential velocity, where the computation captures correctly the evolution outside the central region. The prediction is improved in the survey section S2 as well, given the inherent limitation due to the actual three-dimensional shape of the draft tube.

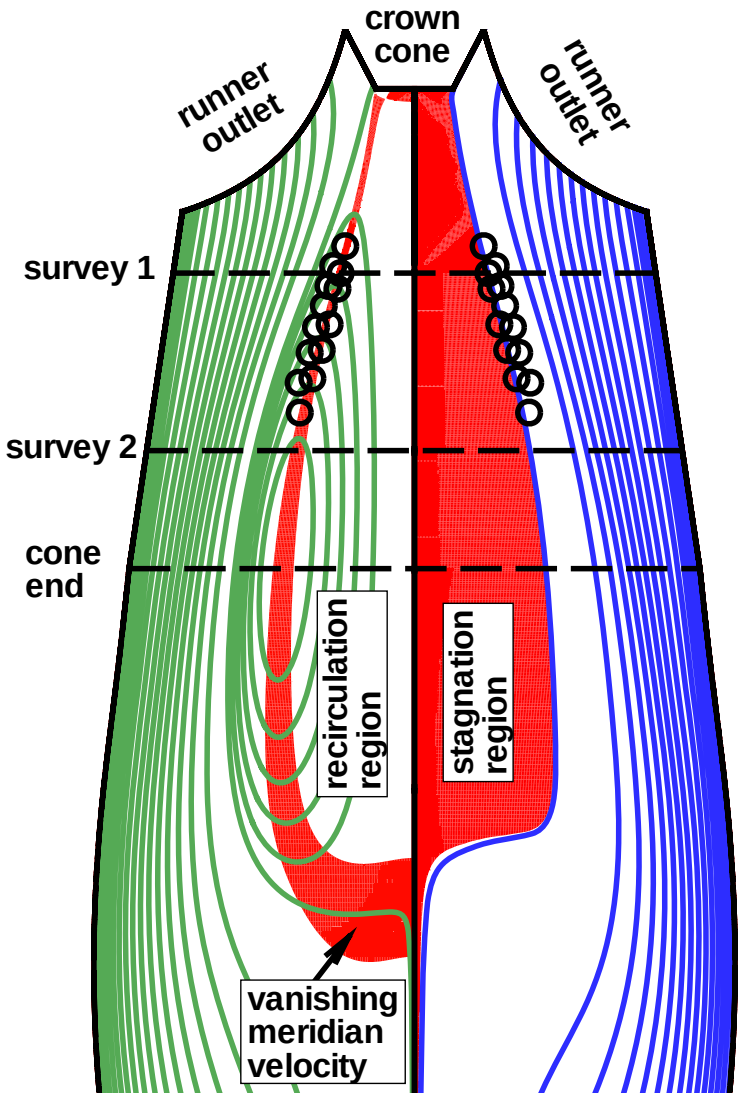

Fig. 5 Streamline pattern and the location of the vortex rope. Numerical results for axisymmetric turbulent flow model without SRM (left half-plane and with SRM (right half-plane).

A further assessment of the axisymmetric swirling flow model is presented in Figure 5, where the streamline pattern in a meridian half-plane is shown for the velocity field computed without (left half-plane) and with (right half-plane) the SRM. Experimental data extracted from PIV investigations of Iliescu et al. [14] provide the vortex rope locus in a meridian half plane, as shown with circles in Figure 5.

When using the SRM, the results shown in the right-hand meridian half-plane from Fig. 5 provide a well defined central stagnant region (shaded in red) with the vortex rope located right on the boundary with the main stream. This result is also supported by the PIV investigation of the velocity field in the straight draft tube of a pump-turbine [19].

If viscosity were neglected, then the corresponding steady axisymmetric Euler equations reduce to the Bragg-Hawthorne equation for the streamfunction ψ, [20]. This equation contains two generating functions deriving from the Kelvin's and Bernoulli's theorems. According to Kelvin's theorem, the circulation function should remain constant on a particular streamsurface $\psi = \text{constant}$, thus we have $rV_\theta = C(\psi)$. According to Bernoulli's theorem, the total specific energy, or total pressure, should also remain constant on a streamsurface, i.e. $p/\rho + V^2/2 = E(\psi)$.

Both circulation and total pressure are plotted dimensionless in Figure 6 versus the normalized streamfunction in four sections: inlet, survey S1 and S2, and cone outlet. The total specific energy is made dimensionless by defining the total pressure coefficient $c_{p\,\text{tot}} \equiv \left(p_{\text{tot}} - \overline{p}_{\text{tot}}^{\text{inlet}}\right)/(\rho g H)$, with $\overline{p}_{\text{tot}}^{\text{inlet}}$ the mass weighed average of the total pressure on the inlet section. Using the normalized streamfunction in the abscissa we have the direct indication of the discharge fraction.

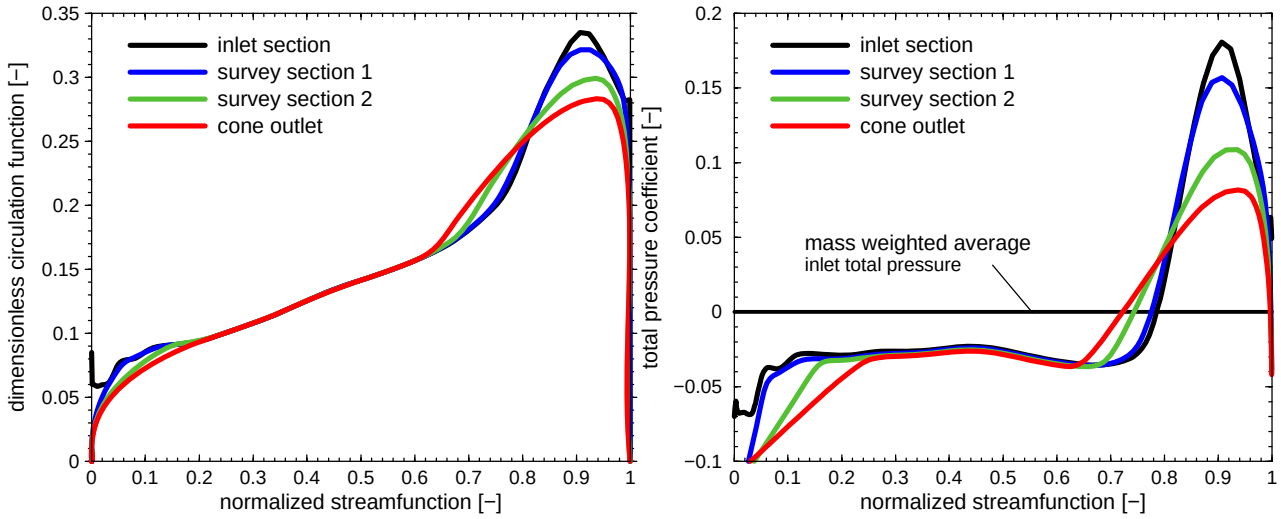

Fig. 6 Dimensionless circulation function (left) and total pressure coefficient (right), respectively, versus the normalized streamfunction.

As expected, the viscous dissipation leads to decay in both circulation and total specific energy as the flow evolves downstream from the inlet section to the cone outlet. The plots in Figure 6 correspond to the flow computed with SRM (streamline pattern in right-hand side of Figure 5), and clearly show the circulation and specific energy content of the main flow. For example, the circulation increases linearly from the crown toward the band, with an excess near the band most likely due to the development of the interblade vortex, [16]. The specific energy is initially practically constant for more than ¾ of the discharge close to the crown, but significantly overshoots the average value for ¼ of the discharge close to the band. These distributions depend on the runner blade design, and can be considered as characteristics of the swirling flow downstream a Francis runner operated at partial discharge. One can also observe in Figure 6 that the specific energy decreases rapidly both near the wall (solid boundary) and near the central stagnant region (fluid boundary). In the middle of the main stream there is little decay in both circulation and specific energy.

4. Conclusions

The main conclusion of the present investigations is that the axisymmetric turbulent swirling flow model can be reliably employed to recover the circumferentially averaged flowfield in the case of the three-dimensional, unsteady swirling flow with precessing vortex rope encountered in the draft tube cone of Francis turbines operated at partial discharge. When adding the Stagnant Region Model (SRM) to the axisymmetric swirling flow solver from the FLUENT commercial code the numerical results are in very good agreement with the measured axial and circumferential velocity profiles, and confirms previous models with respect to the vortex rope location. Moreover, since a 2D numerical simulation is performed, the computing time and resources are at least two orders of magnitude less than a full 3D unsteady flow simulation. As a result, one can use the axisymmetric swirling flow model within parametric studies and optimization procedures in order to either adjust the blade design or to analyze various approaches for mitigating the vortex rope. The elimination of the central stagnant region is also a good indicator for the success of such approaches.

Due to its inherent simplifications, the axisymmetric swirling flow model provides a steady average flow picture for a highly unsteady phenomenon. As a result, one cannot assess directly the level of pressure fluctuations. The presence and extent of the vortex rope can be only indirectly inferred. At this point, a stability study of the steady axisymmetric swirling flow could provide a better assessment of the helical vortex development. However, the development and extent of the central stagnant region could be reduced by optimizing the runner design, thus mitigating the vortex rope and extending the operating range of Francis turbines with acceptable pressure fluctuations.

By examining the specific energy content of the swirling flow downstream a Francis runner operated at partial discharge, we show that there is an important excess near the band, with respect to the average value. On the other hand, a specific energy deficit is developed near the crown and further downstream in the central stagnant region. As a result, a possible flow control approach

for mitigating the vortex rope should re-direct the excess of specific energy from the cone wall toward the central region, thus reducing or eliminating the stagnant region.

5. Appendix.

User Defined Function for the Stagnation Region Model (SRM) Implementation in FLUENT

```
#include "udf.h"
DEFINE_EXECUTE_AT_END(stagnation)
/*
DEFINE EXECUTE AT END is a general-purpose macro that is executed at the end of an
iteration in a steady state run, or at the end of a time step in a transient run.
One can use DEFINE EXECUTE AT END to calculate quantities at these particular times.
Note that one does not have to specify whether the execute-at-end UDF gets executed
at the end of a time step or at the end of an iteration. This is done automatically when
selecting the steady or unsteady time method in FLUENT model.
*/
{
Domain *domain;
Thread *thread;
cell_t  cell;
real axvel, radvel;
domain=Get_Domain(1); /* returns the fluid domain pointer */

thread_loop_c(thread,domain) /* loop over all cells threads in a given domain*/
    {
    begin_c_loop(cell,thread)
        axvel = C_U(cell,thread); /* get the axial velocity value */
        radvel = C_V(cell,thread); /* get the radial velocity value */
        if (axvel < 0.0) /* stagnation condition: reverse meridian velocity */
           {
             C_U(cell,thread) = -axvel;
             C_V(cell,thread) = -radvel;
             C_W(cell,thread)=0.0;
           }
    end_c_loop(cell,thread)
    }
   printf("Reverse backflow meridian velocity \n");
}
```


Acknowledgments

The authors take this opportunity to thank the partners in the FLINDT Project Eureka No. 1625, Alstom Hydro, Electricité de France, GE Hydro, VA Tech Hydro, Voith-Siemens Hydro, PSEL (Funds for Projects and Studies of the Swiss Electric Utilities), and the CTI (Commission for Technology and Innovation) for the experimental data used in the present paper.

Professor R. Susan-Resiga and Dr. S. Muntean were supported by the Romanian National Authority for Scientific Research through the CEEX-C2-M1-1185 "iSMART-Flow", and the Exploratory Research Project 799/2008 granted by the National University Research Council.

Prof. R. Susan-Resiga, Dr. S. Muntean, and Prof. F. Avellan were supported by the Swiss National Science Foundation through the SCOPES Joint Research Project IB7320-110942/1.

The first author would like to acknowledge the fruitful discussions with Dr. Helmut Keck from VA Tech Hydro, during the 2nd IAHR International Meeting of the Workgroup on Cavitation and Dynamic Problems in Hydraulic Machinery and Systems, Timisoara, Romania, Oct. 2007, that triggered the work presented in this paper.

Nomenclature

g	Gravity [m/s^2]	$\boldsymbol{V}, V_z, V_r, V_\theta, V_m$	Velocity vector, and velocity components in axial, radial, circumferential, and meridian directions [m/s]
H	Turbine head [m]	α	Absolute flow angle [dgr]
$\boldsymbol{n}$	Normal unit vector [-]	β	Relative flow angle [dgr]
p, p_{tot}	Static and total pressure, respectively [Pa]	μ, μ_T	Molecular and turbulent dynamic viscosity, respectively, [Pa s]
Q, Q_{opt}	Discharge, and its value at the best efficiency point, respectively [m^3/s]	ρ	Density [kg/m^3]
r, R_{throat}	Radius, and turbine throat radius, respectively [m]	ψ	Stokes streamfunction for axisymmetric flows, [m^3/s]
Sw	Swirl number [-]	Ω	Runner angular speed [rad/s]

References

[1] Escudier, M., 1987, "Confined Vortices in Flow Machinery," Annual Review of Fluid Mechanics, Vol. 19, pp. 27-52.

[2] Zhang, R.-K., Mao, F., Wu, J.-Z., Chen, S.-Y., Wu, Y.-L., and Liu, S.-H., 2009, "Characteristics and Control of the Draft-Tube Flow in Part-Load Francis Turbine," Journal of Fluids Engineering, Vol. 131, 021101-1-13.

[3] Susan-Resiga, R., Ciocan, G. D., Anton, I., and Avellan, F., 2006, "Analysis of the Swirling Flow Downstream a Francis Turbine Runner," Journal of Fluids Engineering, Vol. 128, pp. 177-189.

[4] Ruprecht, A., Helmrich, T., Aschenbrenner, T., and Scherer, T., 2002, "Simulation of Vortex Rope in a Turbine Draft Tube", Proceedings of the 21st IAHR Symposium on Hydraulic Machinery and Systems, Lausanne, Switzerland, Vol. 1, pp. 259-276.

[5] Sick, M., Stein, P., Doerfler, P., White, P., and Braune, A., 2005, "CFD Prediction of the Part-Load Vortex in Francis Turbines and Pump-Turbines," International Journal of Hydropower and Dams, Vol. 12, No. 85.

[6] Stein, P., Sick, M., Doerfler, P., White, P., and Braune, A., 2006, "Numerical Simulation of the Cavitating Draft Tube Vortex in a Francis Turbine," Proceedings of the 23rd IAHR Symposium on Hydraulic Machinery and Systems, Yokohama, Japan, paper F228 (on CD-ROM, ISBN 4-8190-1809-4).

[7] Ciocan, G. D., Iliescu, M. S., Vu, T. C., Nennemann, B., and Avellan, F., 2007, "Experimental Study and Numerical Simulation of the FLINDT Draft Tube Rotating Vortex," Journal of Fluids Engineering, Vol. 129, pp. 146-158.

[8] Susan-Resiga, R., Vu, T. C., Muntean, S., Ciocan, G. D., and Nennemann, B., 2006, "Jet Control of the Draft Tube Vortex Rope in Francis Turbines at Partial Discharge," Proceedings of the 23rd IAHR Symposium on Hydraulic Machinery and Systems, Yokohama, Japan, paper F192 (on CD-ROM, ISBN 4-8190-1809-4).

[9] Olendraru, C., and Sellier, A., 2002, "Viscous effects in the absolute-convective instability of the Batchelor vortex", Journal of Fluid Mechanics, Vol. 459, pp. 371-396.

[10] Szeri, A., and Holmes, P., 1988, "Nonlinear Stability of Axisymmetric Swirling Flows", Philosophical Transactions of the Royal Society of London. Series A, Mathematical and Physical Sciences, Vol. 326, No. 1590, pp. 327-354.

[11] Blackburn, H. M., and Sherwin, S. J., 2004, "Formulation of a Galerkin spectral element – Fourier method for three-dimensional incompressible flows in cylindrical geometries," Journal of Computational Physics, Vol. 197, pp. 759-778.

[12] Alekseenko, S. V., Kuibin, P. A., Okulov, V. L., and Shtork, S. I., 1999, "Helical vortices in swirl flow," Journal of Fluid Mechanics, Vol. 382, pp. 195-243.

[13] Kuibin, P. A., Okulov, V. L., and Pylev, I. M., 2006, "Simulation of Flow Structure in the Suction Pipe of a Hydroturbine by Integral Characteristics," Heat Transfer Research, Vol. 37, No. 8, pp. 675-684.

[14] Iliescu, M. S., Ciocan, G. D., and Avellan, F., 2008, "Analysis of the Cavitating Draft Tube Vortex in a Francis Turbine Using Particle Image Velocimetry Measurements in Two-Phase Flow," Journal of Fluids Engineering, Vol. 130, 021105-1-10.

[15] Avellan, F., 2000, "Flow Investigation in a Francis Draft Tube: The FLINDT Project," Proceedings of the 20th IAHR Symposium on Hydraulic Machinery and Systems, Charlotte, North-Carolina, U.S.A., Paper DES-11.

[16] Avellan, F., 2004, "Introduction to Cavitation in Hydraulic Machinery," 6th International Conference on Hydraulic Machinery and Hydrodynamics, Timişoara, Romania, Scientific Bulletin of the Politehnica University of Timişoara, Transactions on Mechanics, Tom 49(63), Special Issue, pp.11-22.

[17] Shih, T.-H., Liou, W. W., Shabbir, A., Yang, Z., and Zhu, J., 1995, "A New k-ε Eddy Viscosity Model for High Reynolds Number Turbulent Flows – Model Development and Validation," Computer & Fluids, Vol. 24, No. 3, pp. 227-238.

[18] Nishi, M., Matsunaga, S., Okamoto, S,. Uno, M., and Nishitani, K., 1988, "Measurement of Three-dimensional Periodic Flow in a Conical Draft Tube at Surging Condition," in Rohatgi, U. S., at al., (eds.), Flow in Non-Rotating Turbomachinery Components, FED, Vol. 69, pp. 173-184.

[19] Kirschner, O., and Ruprecht, A., 2007, "Vortex Rope Measurement in a Simplified Draft Tube," 2nd IAHR International Meeting of the Workgroup on Cavitation and Dynamic Problems in Hydraulic Machinery and Systems, Timişoara, Romania, Scientific Bulletin of the Politehnica University of Timisoara, Transactions on Mechanics, Tom 52(66), Fasc. 6, pp. 173-184.

[20] Keller, J. J., Egli, W., and Althaus, R., 1988, "Vortex Breakdown as a Fundamental Element of Vortex Dynamcis," Journal of Applied Mathematics and Physics (ZAMP), Vol. 39, pp. 404-440.